



## Determinants of aponeurosis shape change during muscle contraction



Christopher J. Arellano<sup>a,\*</sup>, Nicholas J. Gidmark<sup>a,1</sup>, Nicolai Konow<sup>a</sup>, Emanuel Azizi<sup>b</sup>,  
Thomas J. Roberts<sup>a</sup>

<sup>a</sup> Department of Ecology and Evolutionary Biology, Brown University, Providence, RI 02912, USA

<sup>b</sup> Department of Ecology and Evolutionary Biology, University of California, Irvine, CA 92697, USA

### ARTICLE INFO

#### Article history:

Accepted 18 April 2016

#### Keywords:

Muscle  
Aponeuroses  
Strain  
Tendon  
Elastic

### ABSTRACT

Aponeuroses are sheet-like elastic tendon structures that cover a portion of the muscle belly and act as insertion sites for muscle fibers while free tendons connect muscles to bones. During shortening contractions, free tendons are loaded in tension and lengthen due to the force acting longitudinally along the muscle's line of action. In contrast, aponeuroses increase in length and width, suggesting that aponeuroses are loaded in directions along and orthogonal to the muscle's line of action. Because muscle fibers are isovolumetric, they must expand radially as they shorten, potentially generating a force that increases aponeurosis width. We hypothesized that increases in aponeurosis width result from radial expansion of shortening muscle fibers. We tested this hypothesis by combining *in situ* muscle-tendon measurements with high-speed biplanar fluoroscopy measurements of the turkey's lateral gastrocnemius ( $n=6$ ) at varying levels of isotonic muscle contractions. The change in aponeurosis width during periods of constant force depended on both the amount of muscle shortening and the magnitude of force production. At low to intermediate forces, aponeurosis width increased in direct proportion to fiber shortening. At high forces, aponeurosis width increased to a lesser extent or in some cases, decreased slightly during fiber shortening. Our results demonstrate that forces generated from radial expansion of shortening muscle fibers tend to drive increases in aponeurosis width, whereas longitudinal forces tend to decrease aponeurosis width. Ultimately, it is these two opposing forces that drive changes in aponeurosis width and alter series elastic stiffness during a muscle contraction.

© 2016 Elsevier Ltd. All rights reserved.

### 1. Introduction

Tendinous structures can be categorized as either free tendons or aponeuroses. Free tendons operate in series with muscle fibers and are loaded in tension when muscles produce force along their line of action. Aponeuroses, on the other hand, are sheet-like elastic structures that cover a portion of the muscle belly and acts as an insertion site for muscle fibers (Williams, 1995). Studies of isolated muscles show that these connective tissues can undergo positive strains in more than one direction during a contraction (Azizi and Roberts, 2009; Scott and Loeb, 1995; van Donkelaar et al., 1999). This observation indicates that the mechanical loading of aponeuroses is more complex than that of free tendons.

Materials testing of isolated aponeuroses show that under uniaxial loading in the longitudinal direction (*i.e.* along the line of action of the whole muscle-tendon unit), aponeuroses decrease in

width (Azizi et al., 2009), as expected for a uniaxially loaded material. During a muscle contraction, however, aponeuroses often increase in length and width simultaneously (Azizi and Roberts, 2009). This biaxial strain behavior suggests that some force must act in the transverse direction (orthogonal to the muscle's line of action) to increase aponeurosis width. However, the factors that govern aponeurosis shape change and as a consequence, its elastic mechanical behavior remain unresolved.

We tested the hypothesis that during a muscle contraction, fiber shortening generates the orthogonal force required to increase aponeurosis width. Muscle fibers are isovolumetric and therefore must expand radially as they shorten (Baskin and Paolini, 1967; Rabbany et al., 1994). The radial expansion of shortening muscle fibers may drive the increase in aponeurosis width that has been observed during muscle contractions (Azizi and Roberts, 2009). In a homogenous, isotropic material loaded biaxially, the strain along an axis of loading is determined by the force acting along that axis, the Poisson's ratio, and the force acting along the orthogonal axis (Gere, 2001). Aponeuroses are not isotropic or homogenous (Azizi et al., 2009), but we expected that strains in aponeurosis width would also be governed by a combination of forces acting along the longitudinal and transverse directions.

\* Correspondence to: Department of Ecology and Evolutionary Biology Brown University, Box G-W 02912, United States. Tel.: +401 863 6477.

E-mail address: [arellanoc@gmail.com](mailto:arellanoc@gmail.com) (C.J. Arellano).

<sup>1</sup> Current Affiliation for NJ Gidmark: Biology Department, Knox College, Galesburg, IL 61401, USA

Thus, we predicted that during a shortening muscle contraction, two forces would govern changes in aponeurosis width: (1) force resulting from radial expansion (*i.e.* bulging) of shortening muscle fibers, and (2) force acting along the muscle's longitudinal line of action. Fiber bulging due to shortening should tend to increase aponeurosis width, whereas increases in longitudinal force should tend to decrease aponeurosis width, as expected for a biaxially loaded material. To test this hypothesis, we measured the loading response of the aponeurosis across a wide range of constant force levels to determine the influence of muscle fiber shortening on aponeurosis width.

## 2. Material and methods

Adult, wild turkeys (*Meleagris gallopavo*) were purchased from a licensed breeder and housed in the Animal Care Facilities at Brown University. Animals were provided a commercial poultry diet and water *ad libitum*. The Brown University Institutional Animal Care and Use Committee approved the use of animals and the experimental protocol for this study.

This study combines previously published data (Azizi and Roberts, 2009) with newly collected data for a total of  $n = 6$  animals. The data collected in each experiment used the same X-ray imaging technique to capture the position of radio-opaque markers that tracked aponeurosis shape change in the longitudinal and transverse direction during a muscle contraction. Muscle fiber length change data in Azizi and Roberts (2009) were collected using sonomicrometry while data in the present study were collected using an X-ray imaging technique detailed below.

### 2.1. Muscle preparation and instrumentation

Following established *in situ* methods (Azizi and Roberts, 2009; Gabaldon et al., 2004; Konow and Roberts, 2015; Nelson et al., 2004), animals were first placed under deep anesthesia while small (0.8–1.0 mm diameter) radiopaque markers were surgically implanted along the proximal muscle fiber and into the aponeurosis of the lateral gastrocnemius muscle (LG). The femur and tarsometatarsus were oriented at a 90° angle and rigidly secured to a custom rig (Fig. 1A).

The bony tendon at the distal end of the LG muscle was dissected away from its connection to the free tendons that provides muscle tendon unit attachment onto the tarsometatarsus. The bony tendon was attached to a custom-made clamp and connected to the lever arm of a servo-controlled motor that regulates force and length (Model 310-BLR, Aurora Scientific). To stimulate the muscle, a small bipolar cuff was secured to the tibial branch of the sciatic nerve. Electrical stimuli were used to elicit tetanic muscle contractions (Grass S48, Grass Technologies, West Warwick, RI; 0.2 ms rectangular pulses; 100 pulses/s, 100–300 ms train duration). Servomotor measurements of force and length as well as stimulation voltage were collected with a 16-bit A/D converter (Model PCMI0-16, Austin, TX) at 1000 samples per second using custom procedures in IGOR Pro (v6, WaveMetrics, Lake Oswego, OR).

### 2.2. Experimental protocol

The muscle-tendon was first set to a resting length that produced a passive force between 5 and 10 N. Supramaximal stimulus voltage was then determined with a series of twitches and used throughout the rest of the experiment. A series of fixed end contractions at various muscle-tendon lengths were performed to produce a tetanic force-length curve, which was used to identify the optimal length ( $L_o$ ) at which the muscle produced maximum isometric force ( $P_o$ ).

Force control parameters on the servomotor were then adjusted so that isotonic muscle contractions (constant force) were performed at various proportions of  $P_o$ . Under these conditions, the supramaximally stimulated muscle was allowed to generate force until it reached the target force level (Fig. 2A), then the servomotor maintained a constant force by allowing the muscle-tendon unit (Fig. 2B) and muscle fibers (Fig. 2E) to shorten at a relatively constant rate.

### 2.3. Video recordings

*In situ* measurements of muscle force were combined with high-speed biplanar fluoroscopy to capture aponeurosis shape change during a muscle contraction. Radio-opaque marker data in Azizi and Roberts (2009) were recorded at 250 frames/s using two C-arm fluoroscopes (OEC Model 9400) integrated with high-speed cameras (Photron Fastcam 1024 m, Photron Inc. San Diego, CA, USA). The new data were recorded using a custom-built biplanar videography set-up (W. M. Keck Foundation XROMM Facility, Brown University). The system consists of two X-ray tubes (Varian model G-1086), two pulsed X-ray generators (EMD Technologies model EPS 45–80), and two 16" diameter image intensifiers (Dunlee model TH9447QXH590). X-ray imaging parameters were set at 80–85 kVp, 160 mA, in

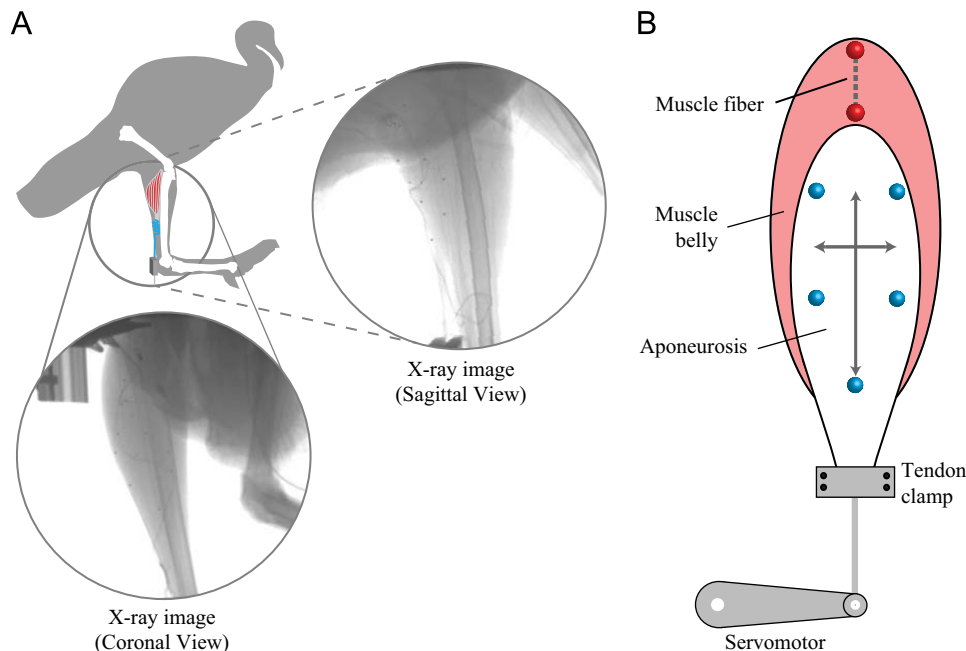


**Fig. 1.** An *in-situ* preparation combined with high-speed fluoroscopy quantified the effects of muscle fiber shortening on aponeurosis width during isotonic contractions. (A) The femur and tarsometatarsus of a turkey (gray silhouette) were oriented so that the distal end of the bony tendon of the lateral gastrocnemius (LG) was clamped to a servomotor. Two high-speed biplanar X-ray cameras captured the positions of the radio-opaque markers surgically implanted along the muscle fiber and aponeurosis surface. (B) A schematic illustration showing a coronal plane view of the LG muscle-tendon unit. The three-dimensional marker coordinates were used to quantify changes in muscle fiber length (red markers), aponeurosis length (vertical arrow), and aponeurosis width (horizontal arrow) during isotonic muscle contractions. Light blue markers denote the 3D position of radio-opaque markers implanted at the aponeurosis surface. Note that only these markers are highlighted in the schematic illustration because they were used to quantify the specific variables of interest. (For interpretation of the references to color in this figure legend, the reader is referred to the web version of this article.)

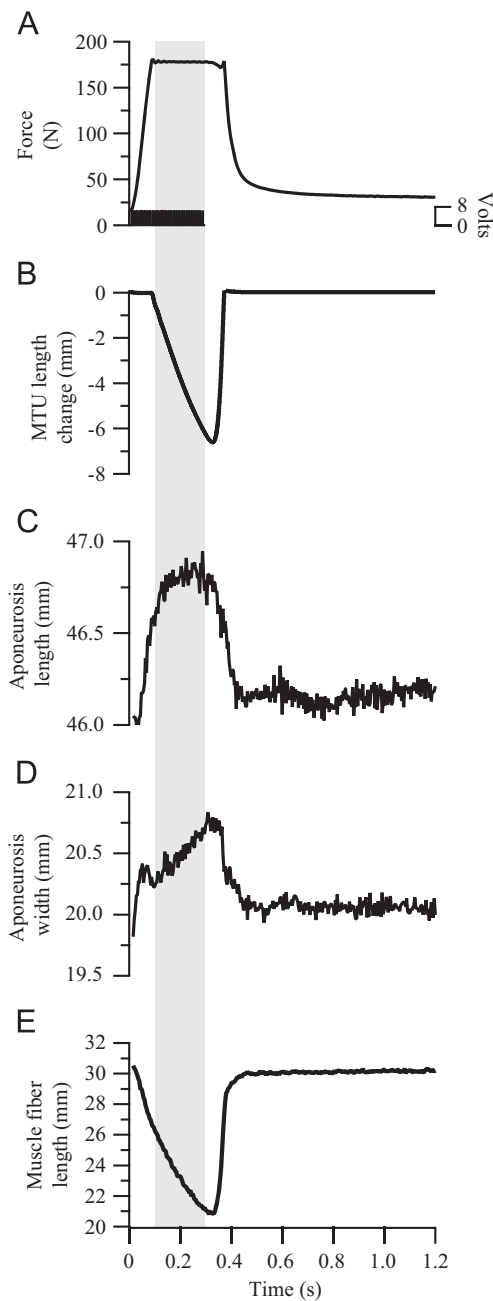


**Fig. 2.** Representative time-series data for an isotonic contraction illustrates that during the period of constant force, fiber shortening coincides with an increase in aponeurosis width. (A) During the period of nerve stimulation, muscle force rises rapidly until reaching a level of 180 N. (B) At this instant, the servomotor allows the muscle-tendon to shorten at a rate that produces a constant force (gray vertical region). During the period of constant force, aponeurosis length (C) remains roughly the same while an increase in aponeurosis width (D) coincides with fiber shortening (E).

continuous mode with an extended dynamic range of 100–180 and an SID of 120 cm. Images were acquired using two high-resolution (1760 × 1760 pixel) Phantom v10 high-speed digital cameras (Vision Research) recording at 250 frames per second and 500  $\mu$ s exposure time.

#### 2.4. Data analysis and statistics

For each contraction, the positions of the radio-opaque markers were tracked following an established marker-based workflow available through XrayProject software (Brainerd et al., 2010; [www.xromm.org](http://www.xromm.org)), which includes image undistortion and volume calibration using direct linear transformation. The precision of the fluoroscopy measurement system for tracking pairwise inter-marker distances has been determined to be better than 0.09 mm (Brainerd et al. 2010). The final

output of the workflow are the 3D coordinates for each radio-opaque marker, which were imported into IGOR Pro and used to quantify changes in proximal fiber length, aponeurosis length, and aponeurosis width during a muscle contraction.

Changes in muscle fiber length were measured using two methods. For four animals (Azizi and Roberts, 2009), instantaneous muscle fiber length was measured using sonomicrometry. For the newly collected data, which includes two animals, muscle fiber length was measured as the inter-marker distance between a pair of radio-opaque markers that ran along a fiber located at the muscle's proximal end (red markers, Fig. 1B). Since biplanar fluoroscopy was used to collect the 3D position of radio-opaque markers implanted on the surface of the aponeurosis surface in both experiments, the same approach was followed to quantify changes in aponeurosis length and width. Aponeurosis length changes (vertical arrow in Fig. 1B) were measured along the midline by quantifying the distance between the position of a midpoint marker located near the proximal region and a single radio-opaque marker (light blue) oriented at the distal region (Fig. 1B). The 3D position of the midpoint marker located at the proximal end of the aponeurosis was calculated from a pair of markers oriented along the same transverse axis. Changes in aponeurosis width (horizontal arrow) were measured by quantifying the distance between a midpoint marker located at the right side and a midpoint marker located at left side of the aponeurosis. For example, the 3D position of the left midpoint marker was calculated from a pair of radio-opaque markers oriented along their own longitudinal axis (Fig. 1B). The same approach was followed for calculating the 3D position of the right midpoint marker. These markers delineated the transverse midline of the aponeurosis. High-frequency noise fluctuations inherent in the muscle fiber length and aponeurosis width measurements were subsequently removed by implementing a smoothing spline algorithm in IGOR Pro (smoothing factor=1; s.d.=0.01–0.1).

The primary focus of the present analyses was on the relation between changes in fiber length and aponeurosis width during the period of constant muscle force. Therefore, these data were transformed into strain measurements by calculating the length change relative to a reference resting length for the proximal fiber and width of the aponeurosis, respectively. Strain for each variable is given by the equations

$$\epsilon_{\text{fiber}} = \frac{-(L_f - L_i)}{L_r} \quad (1)$$

and

$$\epsilon_{\text{aponeurosis width}} = \frac{W_f - W_i}{W_r} \quad (2)$$

where  $L_f$ ,  $W_f$  and  $L_i$ ,  $W_i$  are final and initial fiber length and aponeurosis width, respectively. Reference values for fiber length ( $L_r$ ) and aponeurosis width ( $W_r$ ) were measured in resting muscle at a length that produced approximately 5 N of passive force. The negative sign in Eq. (1) is added to meet the convention that fiber shortening is positive.

We isolated the influence of fiber shortening strain on aponeurosis strain by analyzing the two during the time when the muscle produced a constant force. The ratio of these strains was calculated as

$$\frac{\epsilon_{\text{aponeurosis width}}}{\epsilon_{\text{fiber}}} = \text{strain ratio} \quad (3)$$

The strain ratio expresses the amount of change in aponeurosis width for a given amount of fiber shortening.

To evaluate how strain ratio varied as a function of muscle force, data were pooled from a series of 41 isotonic muscle contractions measured from different LG muscles ( $n=6$ ). The data were fitted in JMP Pro (version 11.20) with a linear least-squares regression analysis with “individual” and its interaction (individual  $\times$  relative force) as covariates. The “individual” term was treated as a random factor in order to account for random variation among LG muscles (Bolker et al., 2009), while the interaction term (individual  $\times$  relative force) accounts for random variation among the series of isotonic contractions measured at different constant force levels. Significance was set at an  $\alpha$  level=0.05. Along with the  $p$  value, the best-fit line, 95% confidence bands, and the adjusted coefficient of determination ( $r_{\text{adj}}^2$ ) are reported in the figures and text.

### 3. Results

All active, tetanic muscle contractions followed a typical pattern of force and tissue mechanical behavior. As the muscle was supramaximally stimulated, force increased rapidly which coincided with muscle fiber shortening and biaxial expansion (longitudinal and transverse) of the aponeurosis (Fig. 2).

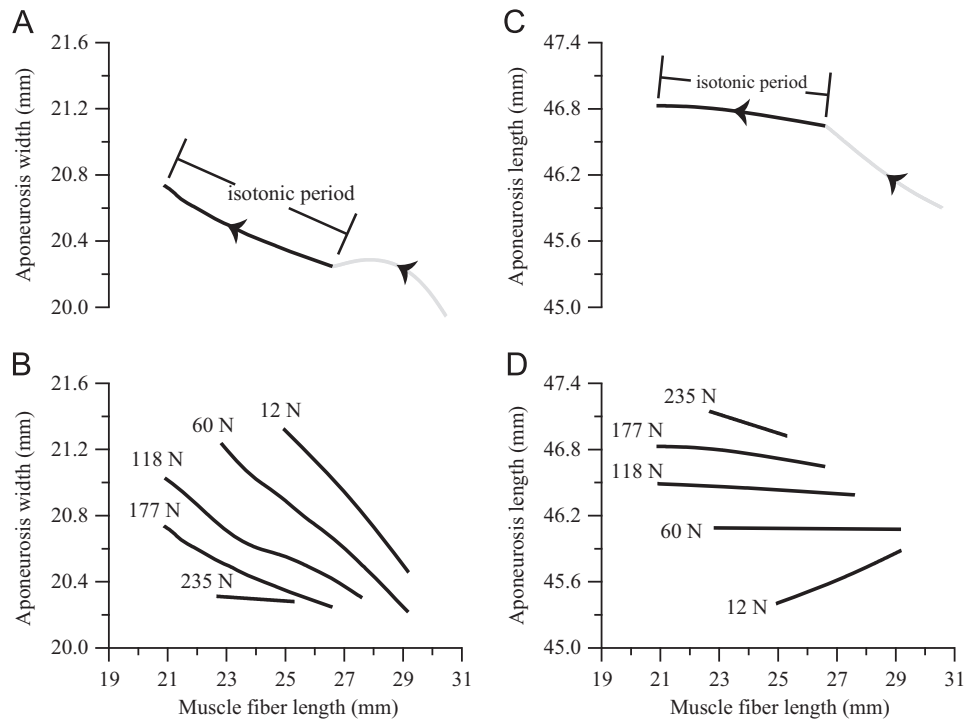


**Fig. 3.** Muscle fiber shortening is accompanied by changes in aponeurosis width during a series of isotonic muscle contractions. Changes in aponeurosis width (A, B) and length (C, D) as a function of fiber shortening. Panels A and C show data for a single contraction, with arrowheads indicating direction of fiber shortening and black lines indicating the period of isotonic muscle contraction. Data from five sample contractions show that during the isotonic period, aponeurosis width increases in proportion to fiber shortening (B), while length is mostly unaffected (D) by fiber shortening. The influence of fiber shortening on aponeurosis width decreases at higher muscle forces (B).

### 3.1. Influence of muscle fiber shortening and force

Across the isotonic contractions measured in this study, aponeurosis width generally increased in direct proportion to fiber shortening (Fig. 3A and B). A representative series of isotonic contractions (Fig. 3B) show that the amount of increase in aponeurosis width for a given amount of fiber shortening also depended on longitudinal force. At higher longitudinal forces, aponeurosis width increased to a lesser extent with fiber shortening. This was the general pattern observed across a series of isotonic contractions measured for each individual LG muscle. For example, when the muscle produced 12 N of constant force, 14.6% of muscle fiber shortening strain coincided with a 4.2% increase in aponeurosis width strain. At 177 N, the same amount of fiber shortening strain coincided with only a 2.7% increase in aponeurosis width strain, representing a 1.6-fold difference. By contrast, there appeared to be little influence of fiber shortening on aponeurosis length (Fig. 3C and D).

### 3.2. Strain ratio vs. relative force

The pattern illustrated in Fig. 3 was consistent across all birds. The influence of longitudinal force on aponeurosis width strain was apparent in the reduced strain ratio values at high force contractions. As a result, the strain ratio (the ratio of aponeurosis width strain for a given amount of fiber shortening strain) decreased as muscle force increased, demonstrating a strong linear relation (Fig. 4). In three individual birds, aponeurosis width strain unexpectedly shifted from its tendency to increase to a tendency to decrease when fibers shortened at constant force contractions ( $P/P_0$ ) above 0.5. For the other three birds, the strain ratio tended toward a value of zero as force approached a maximum value of 1, indicating that increases in aponeurosis width were no longer observed with fiber shortening.

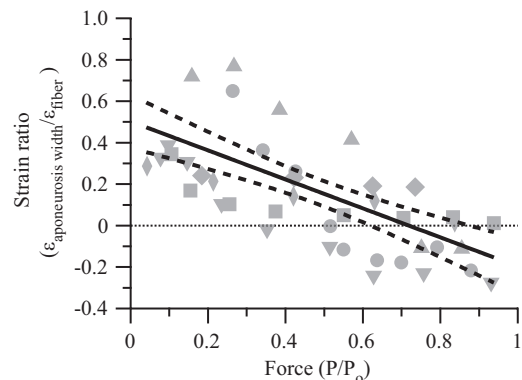


**Fig. 4.** The strain ratio decreases as force increases suggesting that changes in aponeurosis width depend on the interplay between the longitudinal and transverse forces generated during a muscle contraction. Force is measured relative to the muscle's maximum isometric force,  $P_0$ . Positive strain ratios represent contractions where fiber shortening is associated with an increase in aponeurosis width. Negative strain ratios represent contractions where fiber shortening is associated with a decrease in aponeurosis width. Data are pooled from 41 isotonic contractions measured from six LG muscle preparations, which are distinguished by different symbols. Data are fitted with a linear least-squares regression analysis ( $y = -0.70x + 0.50$ ,  $r_{adj}^2 = 0.85$ ,  $p < 0.001$ ). Black solid line represents best-fit line and black dashed lines represent 95% confidence bands.

## 4. Discussion

### 4.1. Determinants of aponeurosis shape change

Our findings support the hypothesis that two forces govern dynamic changes in aponeurosis width during a muscle contraction. Within the range of low to intermediate levels of longitudinal force, aponeurosis width increased in direct proportion to muscle fiber shortening, supporting the hypothesis that radial expansion of muscle fibers produces a force that drives an expansion in

aponeurosis width. In addition, the amount of strain in aponeurosis width for a given amount of fiber shortening strain decreased as muscle force increased, supporting the hypothesis that the force acting along the muscle's longitudinal line of action also influences changes in aponeurosis width. These results demonstrate that the biaxial strain patterns of aponeuroses will depend upon the relative magnitude of these two forces during a shortening muscle contraction.

Uniaxial materials testing indicates that the aponeurosis of the turkey gastrocnemius exhibits elastic behavior in both the longitudinal and transverse directions (Azizi et al., 2009). The aponeurosis is more compliant in the transverse direction, with an elastic modulus that is about one fifth the longitudinal value. The forces associated with an increase in aponeurosis width may be relatively low when compared to longitudinal muscle forces, but they are not negligible. Our results are consistent with the idea that the radial expansion of muscle fibers produces the force needed to drive an increase in aponeurosis width (Fig. 3). Increases in aponeurosis width during shortening contractions have been observed in several different pennate muscles (Azizi and Roberts, 2009; Scott and Loeb, 1995; van Donkelaar et al., 1999). The analyses presented here demonstrate that changes in aponeurosis width for a given amount of muscle fiber shortening decreased as longitudinal force increased. At the highest forces, fiber shortening coincided with zero or even negative aponeurosis width strains (i.e. necking) in some individuals (Fig. 4). The observed effect of longitudinal (muscle line of action) force on aponeurosis width strain is consistent with the expected behavior of a biaxially loaded material (Lanir and Fung, 1974; Treloar, 1975).

#### 4.2. Significance of transverse strain in aponeuroses

These results, coupled with the elastic properties of aponeuroses, suggest that contracting muscle fibers do work in directions orthogonal to the muscle's line of action. Such work presumably results in part from the isovolumetric property of muscle (Baskin and Paolini, 1967; Rabbany et al., 1994), which drives radial expansion of fibers during shortening. We propose that the aponeurosis and possibly intramuscular connective tissue elements resist this expansion, leading to an increase in fluid pressure. This fluid pressure provides the means to transmit forces developed by the contractile element to increase aponeurosis width, and to do work in directions off-axis to the sarcomere. Therefore, the characterization of muscles as simple linear actuators may be overly simplistic. Muscle may be more accurately characterized as multidimensional actuators that produce forces that not only “pull” along the muscle's line of action, but also “push” orthogonal to the muscle's line of action.

How might muscle bulging and its ability to drive aponeurosis shape change influence the mechanical behavior of the aponeurosis? It has been proposed that muscle bulging allows the aponeurosis to act as a variable stiffness spring (Azizi and Roberts, 2009). This idea is illustrated in a comparison of the force-length behavior of aponeurosis undergoing a stretch due to a load caused by (1) an active shortening contraction and (2) a passive lengthening (Fig. 5). As the muscle generates active force, fiber shortening coincides with an increase in aponeurosis width. In contrast, when an external force loads the passive muscle-tendon unit, fiber lengthening coincides with a decrease in aponeurosis width. These two loading patterns (active vs. passive) result in different force-length behavior of the aponeurosis in the longitudinal direction (Fig. 5A). The amount of aponeurosis stretch for a given muscle force during an active contraction is reduced relative to the stretch observed during passive lengthening. For example, at 50 N of active muscle force, the measured segment length of the aponeurosis is 45.7 mm. At the same force during the passive condition, aponeurosis length is 46.3 mm.

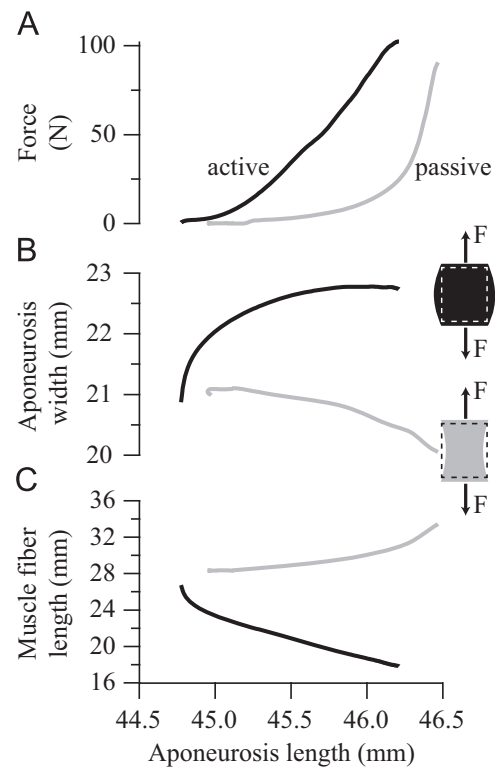


**Fig. 5.** Dynamic muscle shape change modulates the mechanical behavior of the aponeurosis. During active force production in a fixed-end contraction (black lines), the stimulated fibers of the LG muscle produce force (A) and shorten (C) against series elasticity, thus lengthening the aponeurosis (horizontal axis). During this period, radial bulging of the shortening muscle fibers increases the width of the aponeurosis (B). During the passive condition (gray lines), the un-stimulated muscle-tendon unit develops force as it is stretched by a servomotor. During this passive loading, both muscle fibers and the aponeurosis lengthen and therefore, in the absence of fiber shortening and bulging, the width of the aponeurosis decreases (B). A comparison of these two loading patterns (insets in B where dashed lines represent the shape of the aponeurosis prior to loading – depicted by forces,  $F$ , aligned vertically) illustrates that the aponeurosis follows a different force-length behavior profile during active versus passive stretch. This example shows how aponeurosis length is a function of not only muscle longitudinal force, but also on the amount of muscle shortening that translates into an increase in aponeurosis width.

The amount of length change in the elastic tissue elements that are in series with muscle fibers, therefore, is a function of not only the muscle force acting along the line of action, but also of the amount of muscle shortening that translates into an increase in aponeurosis width strain.

#### 4.3. Limitations

Our goal in analyzing the change in aponeurosis dimensions during the constant longitudinal force period of isotonic muscle contractions was to isolate the influence of fiber shortening and longitudinal force on aponeurosis width change. The results indicate that these two variables, fiber shortening and longitudinal force, are important determinants of aponeurosis width change, but it is also possible that other factors may play a role. During the period of force rise in a contraction, the relative timing for achieving a predetermined level of constant force as well as the starting length of the fibers may influence the pattern of aponeurosis shape change. Our contractions did not all start at the same resting length and therefore, initial conditions may explain some of the inter-subject variability in Fig. 4. Such influences may be responsible for the negative aponeurosis strains (necking) observed during fiber shortening, leading to positive strain ratio values in some instances.

#### 4.4. Summary

The findings presented here show that changes in aponeurosis width are governed by (1) transverse forces due to radial expansion of shortening muscle fibers and (2) longitudinal forces directed along the muscle's line of action. The transverse forces due to the radial expansion of shortening muscle fibers will tend to increase aponeurosis width, while longitudinal forces will tend to decrease aponeurosis width. Ultimately, it is the interplay of these two forces that will modulate aponeurosis width during a muscle contraction, and as a consequence, the elastic spring-like behavior of the aponeurosis.

#### Conflict of interest

The authors do not have any financial and personal relationships with other people or organizations that could inappropriately influence (bias) their work.

#### Acknowledgments

We thank Trovov Walker, Drew Schmetterling, and Benjamin Scott for their helpful assistance with digitizing for this project. We are grateful to Christopher V. Anderson for helpful discussions regarding our statistical analyses. The National Institutes of Health research grant [AR055295] to TJR supported this research.

#### References

- Azizi, E., Halenda, G.M., Roberts, T.J., 2009. Mechanical properties of the gastrocnemius aponeurosis in wild turkeys. *Integr. Comp. Biol.* 49, 51–58.
- Azizi, E., Roberts, T.J., 2009. Biaxial strain and variable stiffness in aponeuroses. *J. Physiol.* 587, 4309–4318.
- Baskin, R.J., Paolini, P.J., 1967. Volume change and pressure development in muscle during contraction. *Am. J. Physiol.* 213, 1025–1030.
- Bolker, B.M., Brooks, M.E., Clark, C.J., Geange, S.W., Poulsen, J.R., Stevens, M.H., White, J.S., 2009. Generalized linear mixed models: a practical guide for ecology and evolution. *Trends Ecol. Evol.* 24, 127–135.
- Brainger, E.L., Baier, D.B., Gatesy, S.M., Hedrick, T.L., Metzger, K.A., Gilbert, S.L., Crisco, J.J., 2010. X-ray reconstruction of moving morphology (XROMM): precision, accuracy and applications in comparative biomechanics research. *J. Exp. Zool. A Ecol. Genet. Physiol.* 313, 262–279.
- Gabaldon, A.M., Nelson, F.E., Roberts, T.J., 2004. Mechanical function of two ankle extensors in wild turkeys: shifts from energy production to energy absorption during incline versus decline running. *J. Exp. Biol.* 207, 2277–2288.
- Gere, J.M., 2001. Analysis of stress and strain. In: *Mechanics of Materials*, 5th ed., Brooks/Cole, Division of Thomson Learning, Pacific Grove, CA, p. 926.
- Konow, N., Roberts, T.J., 2015. The series elastic shock absorber: tendon elasticity modulates energy dissipation by muscle during burst deceleration. *Proc. Biol. Sci.* 282, 20142800.
- Lanir, Y., Fung, Y.C., 1974. Two-dimensional mechanical properties of rabbit skin. II. Experimental results. *J. Biomech.* 7, 171–182.
- Nelson, F.E., Gabaldon, A.M., Roberts, T.J., 2004. Force-velocity properties of two avian hindlimb muscles. *Comp. Biochem. Physiol. A Mol. Integr. Physiol.* 137, 711–721.
- Rabbany, S.Y., Funai, J.T., Noordergraaf, A., 1994. Pressure generation in a contracting myocyte. *Heart Vessel.* 9, 169–174.
- Scott, S.H., Loeb, G.E., 1995. Mechanical properties of aponeurosis and tendon of the cat soleus muscle during whole-muscle isometric contractions. *J. Morphol.* 224, 73–86.
- Treloar, L.R.G., 1975. *The Physics of Rubber Elasticity*, 3rd ed. Oxford University Press.
- van Donkelaar, C.C., Willems, P.J.B., Muijtjens, A.M.M., Drost, M.R., 1999. Skeletal muscle transverse strain during isometric contraction at different lengths. *J. Biomech.* 32, 755–762.
- Williams, P.L., 1995. *Gray's Anatomy*. Churchill Livingstone, New York, pp. 749–789.